Towards mapping CSF volume change at high resolutions at 7T

Stephanie Swegle[1], Renzo Huber[1], Rüdiger Stirnberg[2], Javier Gonzalez-Castillo[1], Peter Molfese[1], Linqing Li[1], Catherine Walsh[1], A. Tyler Morgan[1], Peter A. Bandettini[1]

[1]NIH, Bethesda, MD, United States, 20892
[2]German Center for Neurodegenerative Diseases (DZNE), Bonn, Germany

ISMRM 2025
May 12th, 2025
Session: Neurofluids: Techniques & Applications, #0018

Declaration of Financial Interests or Relationships

Speaker Name: Stephanie Swegle

I have no financial interests or relationships to disclose with regard to the subject matter of this presentation.

Background on studying cerebrospinal fluid (CSF)

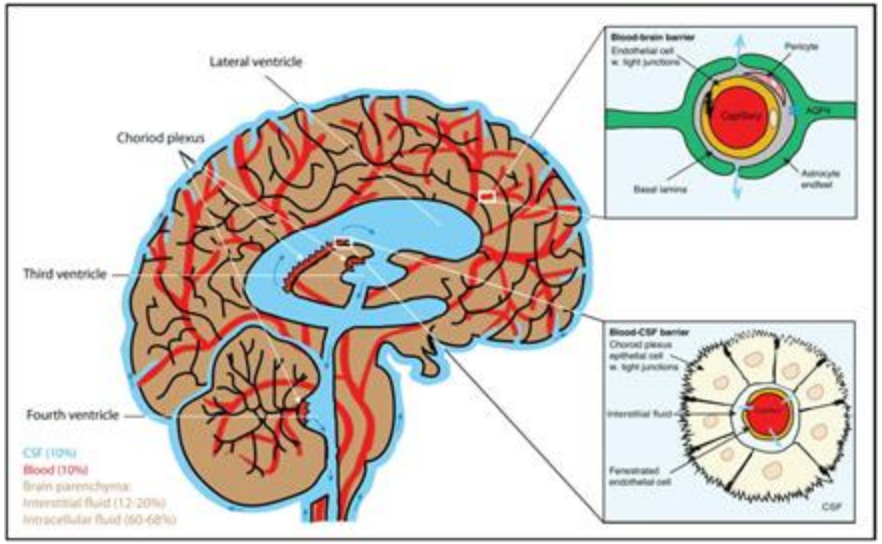

fluid compartments of the brain (Jessen, 2015)

- CSF removes waste and toxins in the brain, especially during sleep
- CSF *flow*: commonly used (Fultz, 2019; Kim, 2022; Grubb, 2019; Gonzalez-Castillo, 2022)
  - but challenged by low velocities, limited imaging coverage, and directional dependencies
  - *Volume* may be more straightforwardly measured
- Contributor and contaminant in VASO (Scouten & Constable, 2008)

We use a VASO-like inversion recovery (IR) sequence to capture CSF volume changes, independent of dynamic changes in CBV and BOLD

Methods

- 7T (N=12 sessions at 7T (Siemens, Germany), 8Tx/32Rx head coil (Nova, USA))
- Multi-echo, multi-inversion
- 3D-EPI with Skipped-CAIPI (Stirnberg, 2021)

- Representative values:
  - TE1/TE2/TE3=9/29/49ms
  - TI1/TI2/TI3=731/1573/2416ms

- Bloch modeling (Huber, 2014; Ivanov, 2013; Donahue, 2011):
  - Assumed T1 values GM/blood/CSF = 1950/2100/4000ms
  - Assumed T2* values GM/blood/CSF/WM = 33.2/37.5/4000/26.815ms

- 12-14 minute block design (30sec blocks) with flashing checkerboards

- Physiological recording to track changes in respiration (Aktas, 2019) (BIOPAC) and in-scanner eye tracking (EyeLink-1000Plus, SR-Research) were done simultaneously to fMRI

- Sample scan parameters (high resolution): 0.8mm iso, 12 slices, TR_{IR}= 3s, TR_{vol}=8.8s
- Sample scan parameters (whole brain **GRAPPA 21**): 2.6mm iso, 80 slices, TR_{IR}= 2.5s, TR_{vol}=2.5s

3D-EPI sampling scheme, segmentation across IR-cycles and 2 phase encoding dimensions

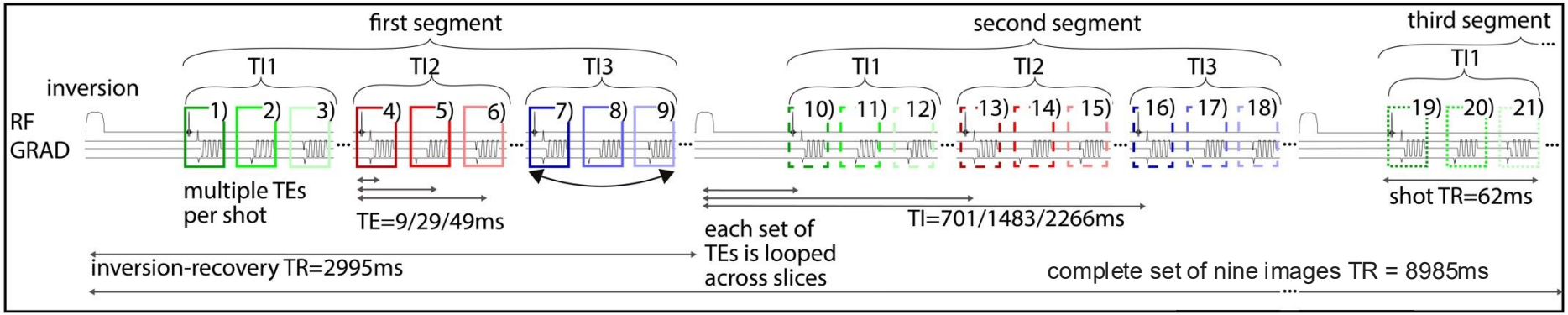

Grouping of 27 shots, sub-sampled data to nine echo planar k-space sets/volumes

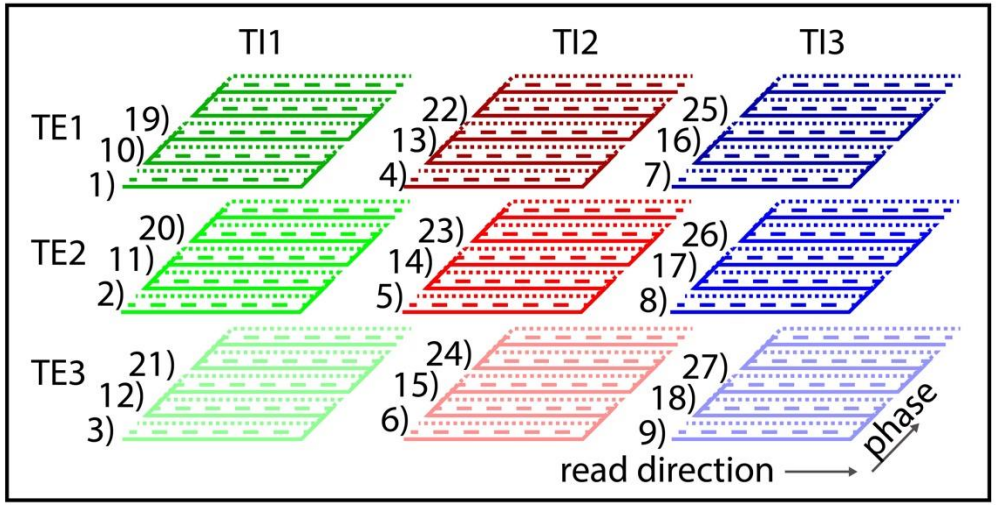

Looping structure from: Stirnberg, et al., 2019. ISMRM #4420

Using CSF's specific relaxation "fingerprint" to separate CSF from CBV and BOLD

CSF is nulled at around TI1

CBV is nulled at around TI2

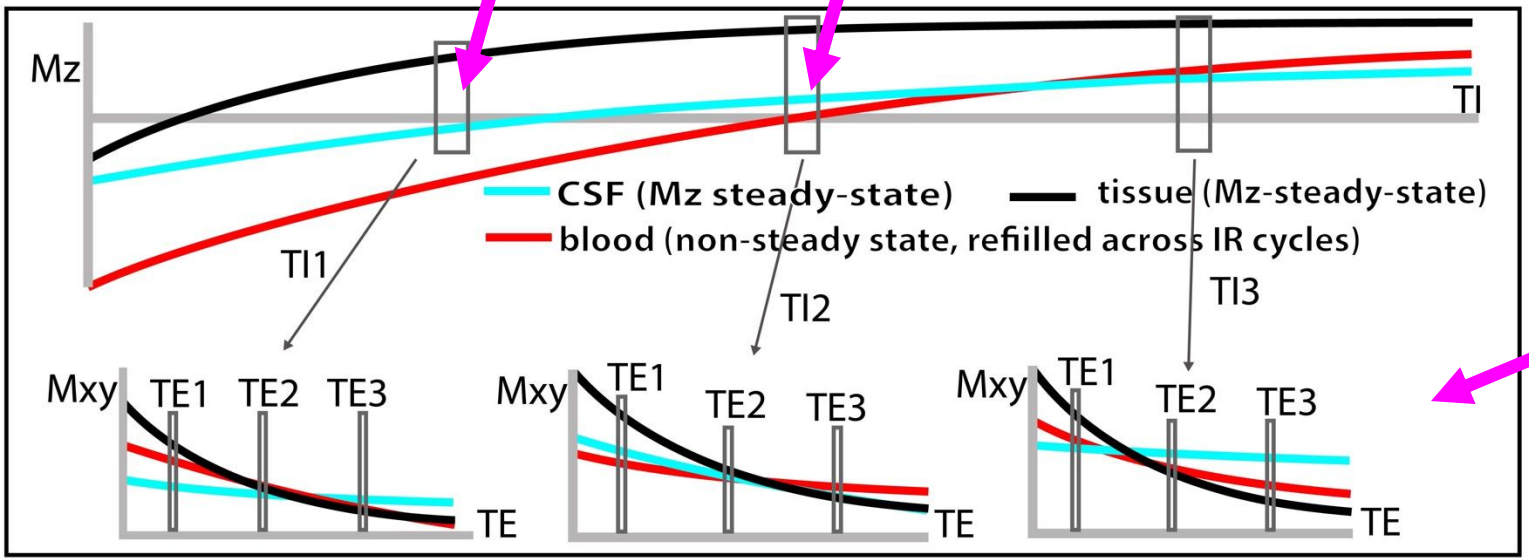

Capturing T2*

Segmentation across IR cycles + advanced readout acceleration (FRISGO, Huber et al., **#1262**) is needed to capture dynamics of inversion recovery

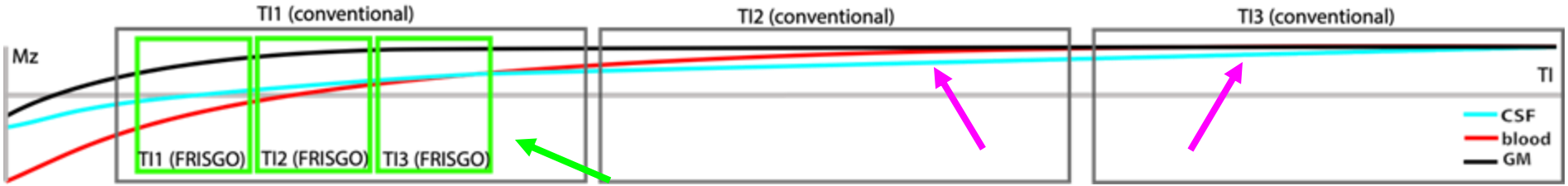

capturing contrast

Conventional EPI is not fast enough to fully capture multi-exponential T1 relaxation

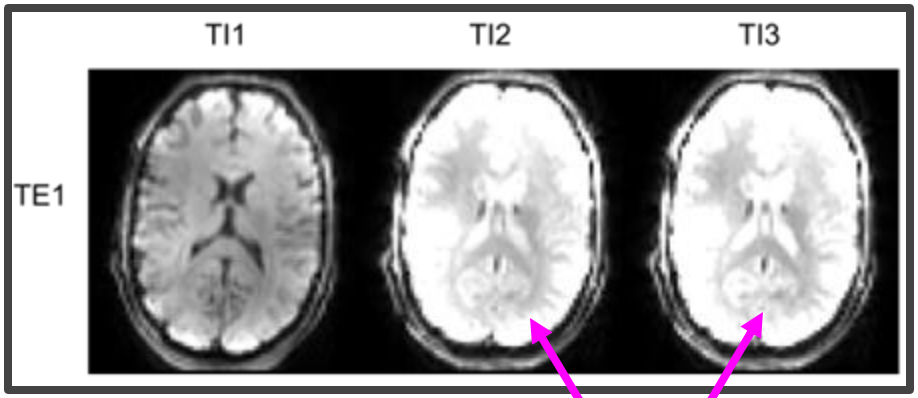

no meaningful T1 contrast

FRISGO (Huber et al., **#1262**) can capture multiple whole brain multi-echo images in time scales of T1

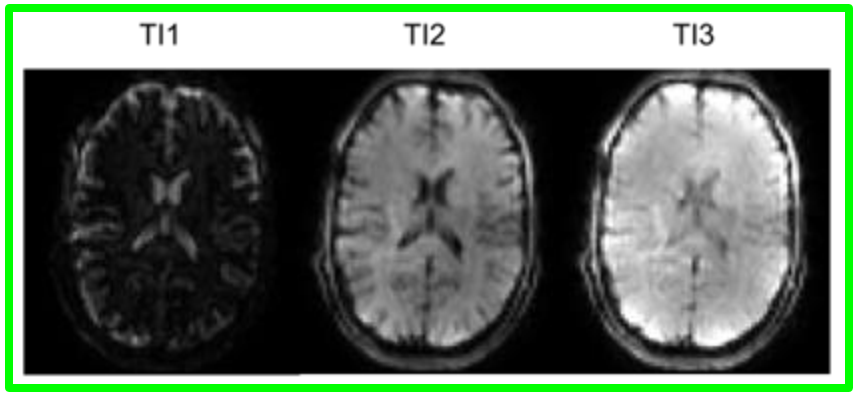

Now, can capture the relevant T1-relaxation in the range of TIs that separates CSF and blood

Bloch Modeling

$$S(TI_1, TE_1, vol) =$$
$$CSF_{vol} * \left[1 - e^{-TI_1/T_{1,CSF}} - \left(M_{CSF}(t=0)\right)e^{-TI_1/T_{1,CSF}}\right] e^{-TE_1/T^*_{2,CSF}} +$$
$$GM_{vol} * \left[1 - e^{-TI_1/T_{1,GM}} - \left(M_{GM}(t=0)\right)e^{-TI_1/T_{1,GM}}\right] e^{-TE_1/T^*_{2,GM}} +$$
$$WM_{vol} * \left[1 - e^{-TI_1/T_{1,WM}} - \left(M_{WM}(t=0)\right)e^{-TI_1/T_{1,GM}}\right] e^{-TE_1/T^*_{2,WM}} +$$
$$CBV * \left[1 - e^{-TI_1/T_{1,blood}} - \left(M_{blood}(t=0)\right)e^{-TI_1/T_{1,blood}}\right] e^{-TE_1/T^*_{2,blood}}$$

$$S(TI_2, TE_1, vol) =$$
$$CSF_{vol} * \left[1 - e^{-TI_2/T_{1,CSF}} - \left(M_{CSF}(t=0)\right)e^{-TI_2/T_{1,CSF}}\right] e^{-TE_1/T^*_{2,CSF}} +$$
$$GM_{vol} * \left[1 - e^{-TI_2/T_{1,GM}} - \left(M_{GM}(t=0)\right)e^{-TI_2/T_{1,GM}}\right] e^{-TE_1/T^*_{2,GM}} +$$
$$WM_{vol} * \left[1 - e^{-TI_2/T_{1,WM}} - \left(M_{WM}(t=0)\right)e^{-TI_2/T_{1,GM}}\right] e^{-TE_1/T^*_{2,WM}} +$$
$$CBV * \left[1 - e^{-TI_2/T_{1,blood}} - \left(M_{blood}(t=0)\right)e^{-TI_2/T_{1,blood}}\right] e^{-TE_1/T^*_{2,blood}}$$

$$S(TI_3, TE_1, vol) =$$
$$CSF_{vol} * \left[1 - e^{-TI_3/T_{1,CSF}} - \left(M_{CSF}(t=0)\right)e^{-TI_3/T_{1,CSF}}\right] e^{-TE_1/T^*_{2,CSF}} +$$
$$GM_{vol} * \left[1 - e^{-TI_3/T_{1,GM}} - \left(M_{GM}(t=0)\right)e^{-TI_3/T_{1,GM}}\right] e^{-TE_1/T^*_{2,GM}} +$$
$$WM_{vol} * \left[1 - e^{-TI_3/T_{1,WM}} - \left(M_{WM}(t=0)\right)e^{-TI_3/T_{1,GM}}\right] e^{-TE_1/T^*_{2,WM}} +$$
$$CBV * \left[1 - e^{-TI_3/T_{1,blood}} - \left(M_{blood}(t=0)\right)e^{-TI_3/T_{1,blood}}\right] e^{-TE_1/T^*_{2,blood}}$$

$$S(TI_1, TE_2, vol) =$$
$$CSF_{vol} * \left[1 - e^{-TI_1/T_{1,CSF}} - \left(M_{CSF}(t=0)\right)e^{-TI_1/T_{1,CSF}}\right] e^{-TE_2/T^*_{2,CSF}} +$$
$$GM_{vol} * \left[1 - e^{-TI_1/T_{1,GM}} - \left(M_{GM}(t=0)\right)e^{-TI_1/T_{1,GM}}\right] e^{-TE_2/T^*_{2,GM}} +$$
$$WM_{vol} * \left[1 - e^{-TI_1/T_{1,WM}} - \left(M_{WM}(t=0)\right)e^{-TI_1/T_{1,GM}}\right] e^{-TE_2/T^*_{2,WM}} +$$
$$CBV * \left[1 - e^{-TI_1/T_{1,blood}} - \left(M_{blood}(t=0)\right)e^{-TI_1/T_{1,blood}}\right] e^{-TE_2/T^*_{2,blood}}$$

$$S(TI_2, TE_2, vol) =$$
$$CSF_{vol} * \left[1 - e^{-TI_2/T_{1,CSF}} - \left(M_{CSF}(t=0)\right)e^{-TI_2/T_{1,CSF}}\right] e^{-TE_2/T^*_{2,CSF}} +$$
$$GM_{vol} * \left[1 - e^{-TI_2/T_{1,GM}} - \left(M_{GM}(t=0)\right)e^{-TI_2/T_{1,GM}}\right] e^{-TE_2/T^*_{2,GM}} +$$
$$WM_{vol} * \left[1 - e^{-TI_2/T_{1,WM}} - \left(M_{WM}(t=0)\right)e^{-TI_2/T_{1,GM}}\right] e^{-TE_2/T^*_{2,WM}} +$$
$$CBV * \left[1 - e^{-TI_2/T_{1,blood}} - \left(M_{blood}(t=0)\right)e^{-TI_2/T_{1,blood}}\right] e^{-TE_2/T^*_{2,blood}}$$

$$S(TI_3, TE_2, vol) =$$
$$CSF_{vol} * \left[1 - e^{-TI_3/T_{1,CSF}} - \left(M_{CSF}(t=0)\right)e^{-TI_3/T_{1,CSF}}\right] e^{-TE_2/T^*_{2,CSF}} +$$
$$GM_{vol} * \left[1 - e^{-TI_3/T_{1,GM}} - \left(M_{GM}(t=0)\right)e^{-TI_3/T_{1,GM}}\right] e^{-TE_2/T^*_{2,GM}} +$$
$$WM_{vol} * \left[1 - e^{-TI_3/T_{1,WM}} - \left(M_{WM}(t=0)\right)e^{-TI_3/T_{1,GM}}\right] e^{-TE_2/T^*_{2,WM}} +$$
$$CBV * \left[1 - e^{-TI_3/T_{1,blood}} - \left(M_{blood}(t=0)\right)e^{-TI_3/T_{1,blood}}\right] e^{-TE_2/T^*_{2,blood}}$$

$$S(TI_1, TE_3, vol) =$$
$$CSF_{vol} * \left[1 - e^{-TI_1/T_{1,CSF}} - \left(M_{CSF}(t=0)\right)e^{-TI_1/T_{1,CSF}}\right] e^{-TE_3/T^*_{2,CSF}} +$$
$$GM_{vol} * \left[1 - e^{-TI_1/T_{1,GM}} - \left(M_{GM}(t=0)\right)e^{-TI_1/T_{1,GM}}\right] e^{-TE_3/T^*_{2,GM}} +$$
$$WM_{vol} * \left[1 - e^{-TI_1/T_{1,WM}} - \left(M_{WM}(t=0)\right)e^{-TI_1/T_{1,GM}}\right] e^{-TE_3/T^*_{2,WM}} +$$
$$CBV * \left[1 - e^{-TI_1/T_{1,blood}} - \left(M_{blood}(t=0)\right)e^{-TI_1/T_{1,blood}}\right] e^{-TE_3/T^*_{2,blood}}$$

$$S(TI_2, TE_3, vol) =$$
$$CSF_{vol} * \left[1 - e^{-TI_2/T_{1,CSF}} - \left(M_{CSF}(t=0)\right)e^{-TI_2/T_{1,CSF}}\right] e^{-TE_3/T^*_{2,CSF}} +$$
$$GM_{vol} * \left[1 - e^{-TI_2/T_{1,GM}} - \left(M_{GM}(t=0)\right)e^{-TI_2/T_{1,GM}}\right] e^{-TE_3/T^*_{2,GM}} +$$
$$WM_{vol} * \left[1 - e^{-TI_2/T_{1,WM}} - \left(M_{WM}(t=0)\right)e^{-TI_2/T_{1,GM}}\right] e^{-TE_3/T^*_{2,WM}} +$$
$$CBV * \left[1 - e^{-TI_2/T_{1,blood}} - \left(M_{blood}(t=0)\right)e^{-TI_2/T_{1,blood}}\right] e^{-TE_3/T^*_{2,blood}}$$

$$S(TI_3, TE_3, vol) =$$
$$CSF_{vol} * \left[1 - e^{-TI_3/T_{1,CSF}} - \left(M_{CSF}(t=0)\right)e^{-TI_3/T_{1,CSF}}\right] e^{-TE_3/T^*_{2,CSF}} +$$
$$GM_{vol} * \left[1 - e^{-TI_3/T_{1,GM}} - \left(M_{GM}(t=0)\right)e^{-TI_3/T_{1,GM}}\right] e^{-TE_3/T^*_{2,GM}} +$$
$$WM_{vol} * \left[1 - e^{-TI_3/T_{1,WM}} - \left(M_{WM}(t=0)\right)e^{-TI_3/T_{1,GM}}\right] e^{-TE_3/T^*_{2,WM}} +$$
$$CBV * \left[1 - e^{-TI_3/T_{1,blood}} - \left(M_{blood}(t=0)\right)e^{-TI_3/T_{1,blood}}\right] e^{-TE_3/T^*_{2,blood}}$$

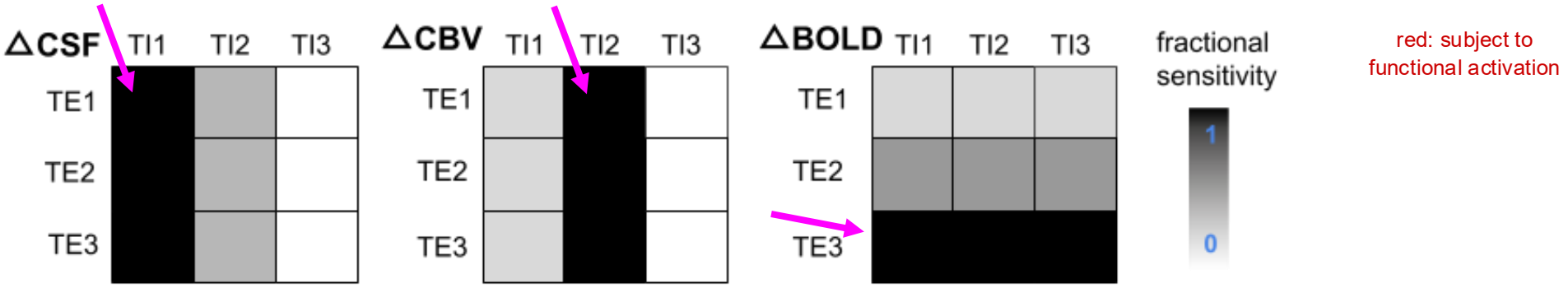

Confirming the method

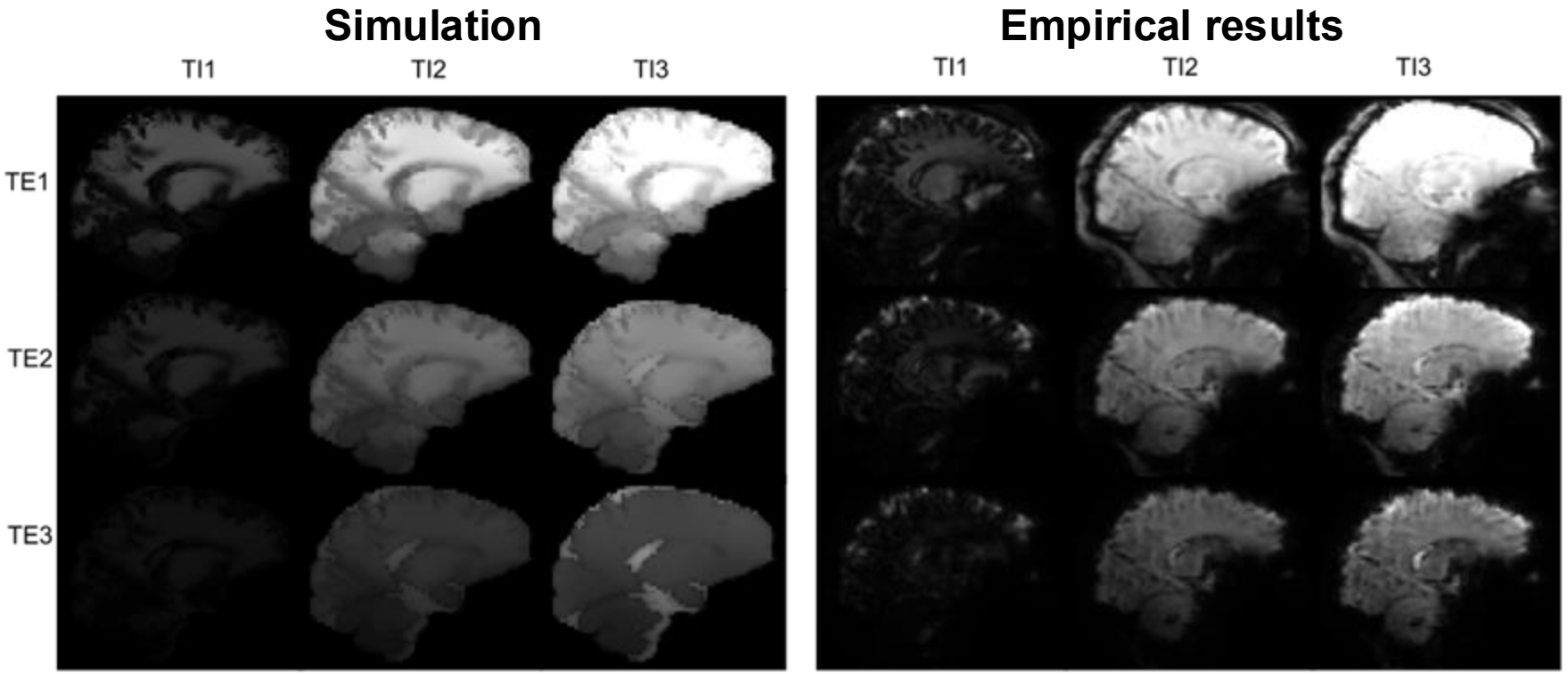

Comparing predicted tissue contrasts and the contrasts seen in the empirical data shows that overall our predictions match the empirical results

Task-locked fluctuations indicate the sequence capturing CSF volume change

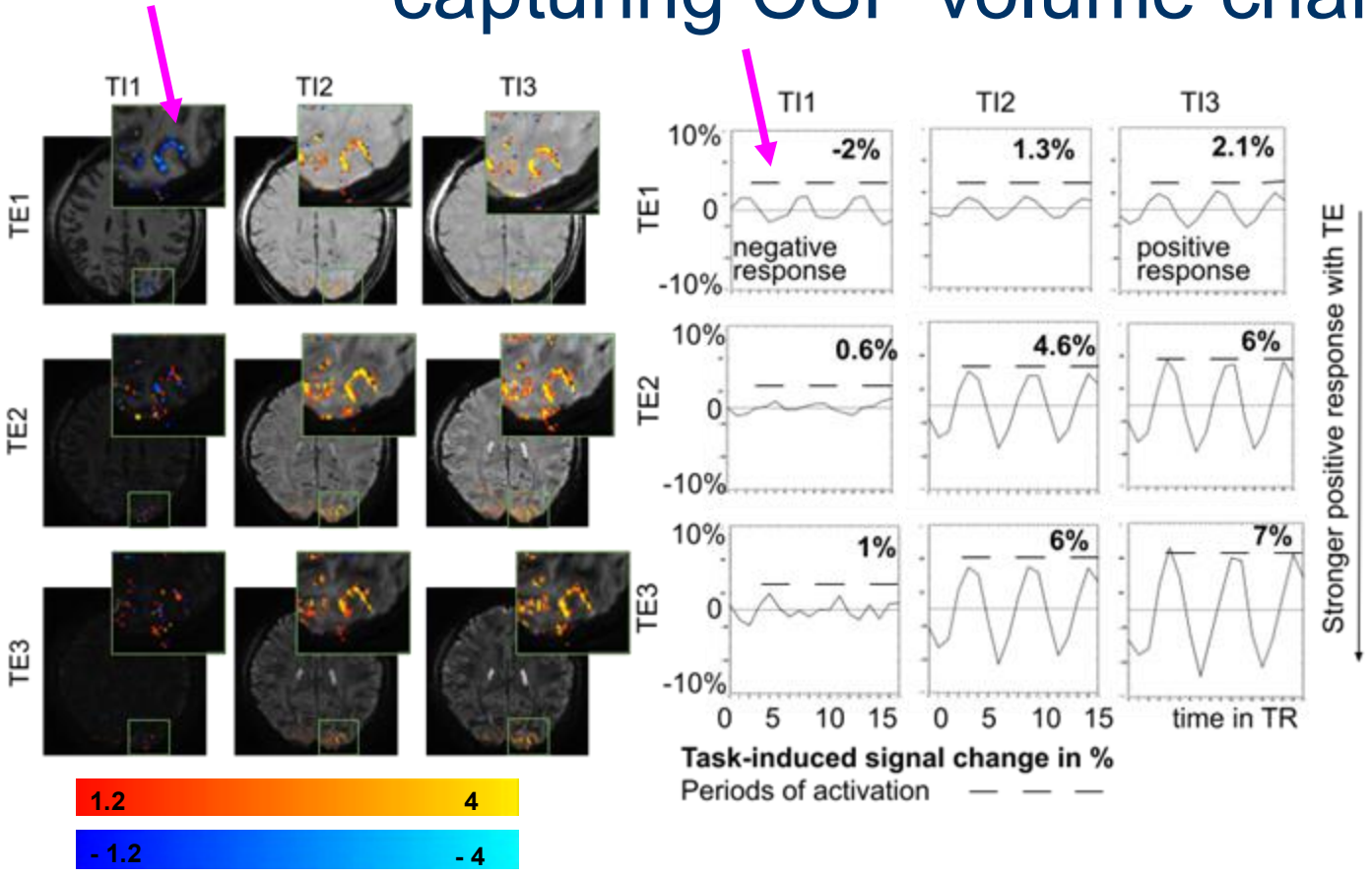

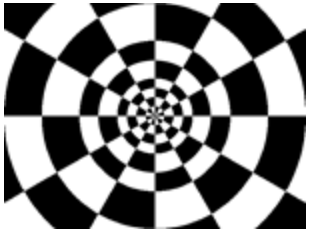

Negative signal changes seen with the early TI, while later TIs resulted in increasingly positive signal changes

Functional responses are stronger at later echo times, as expected from GE-BOLD

Task-locked fluctuations indicate the sequence capturing CSF volume change

Feasibility of 3D whole brain mapping at low resolution (2.6mm) with GRAPPA 21

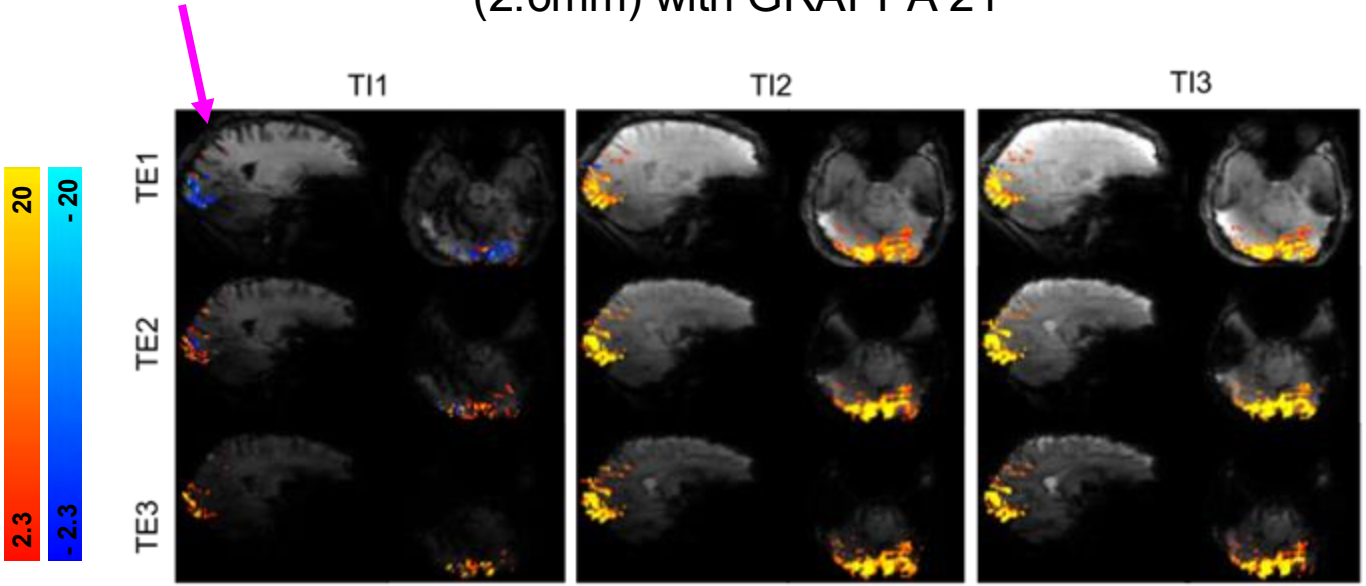

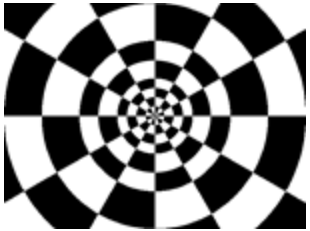

Task-induced activation in the visual cortex can be seen at high resolution, in time courses and at whole brain resolution

Confirmation that this method can spatially map CSF

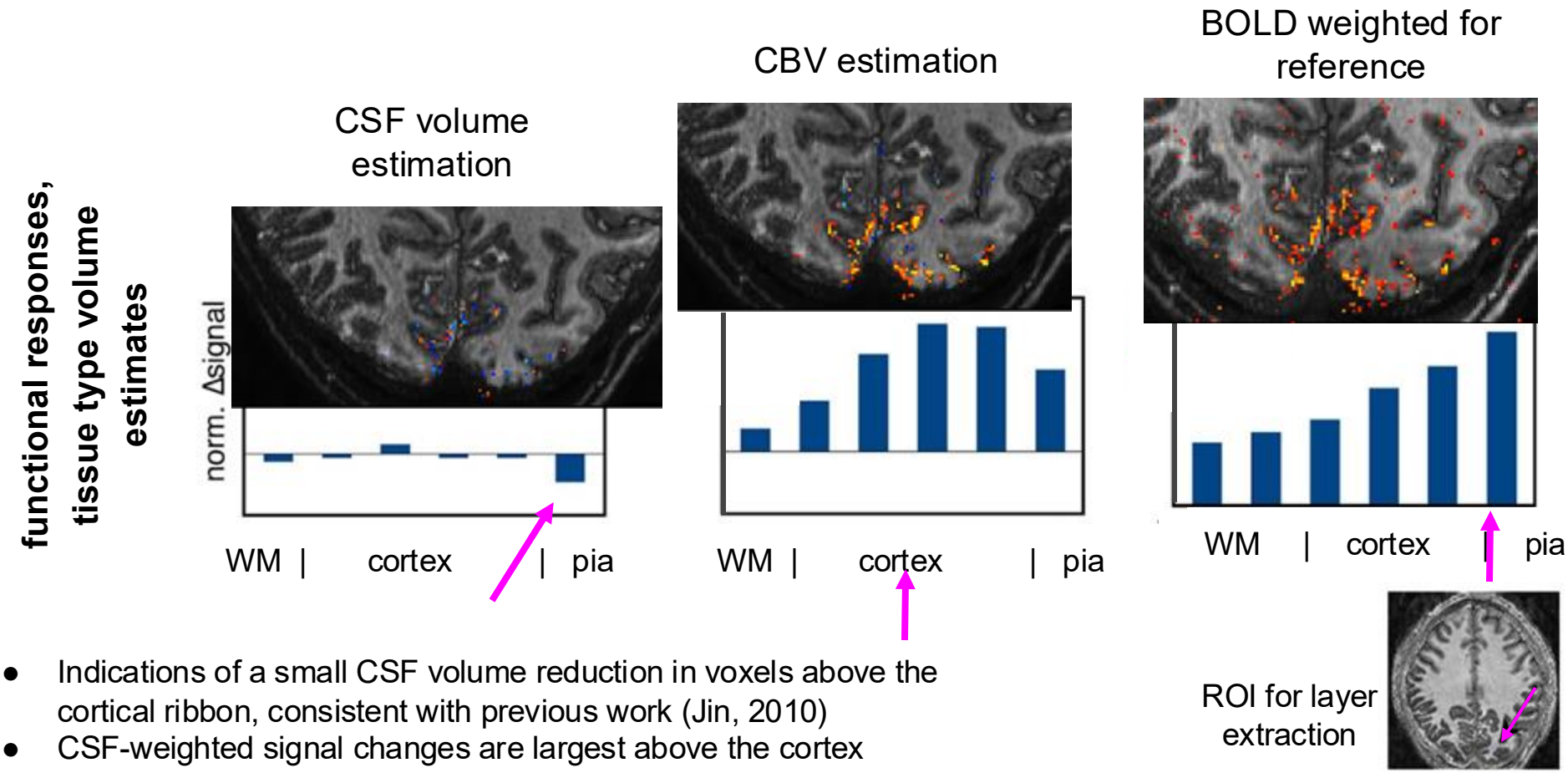

- Indications of a small CSF volume reduction in voxels above the cortical ribbon, consistent with previous work (Jin, 2010)
- CSF-weighted signal changes are largest above the cortex

CSF volume increases as participants get drowsy

Tacking vigilance: Eye tracker for pupil measurement in the scanner room

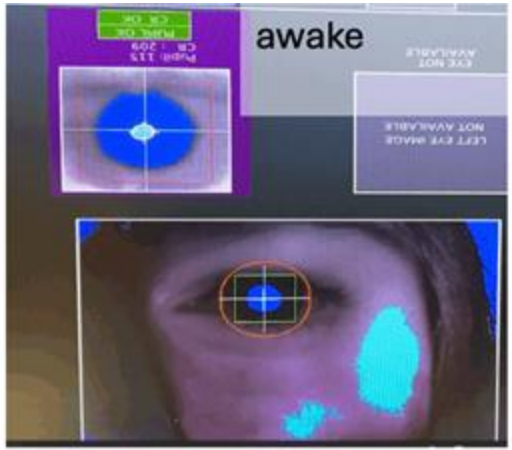

Eye tracking system shown on experimenter

Time course of “sleepy” eyes vs. CSF volume (picked one section of three runs)

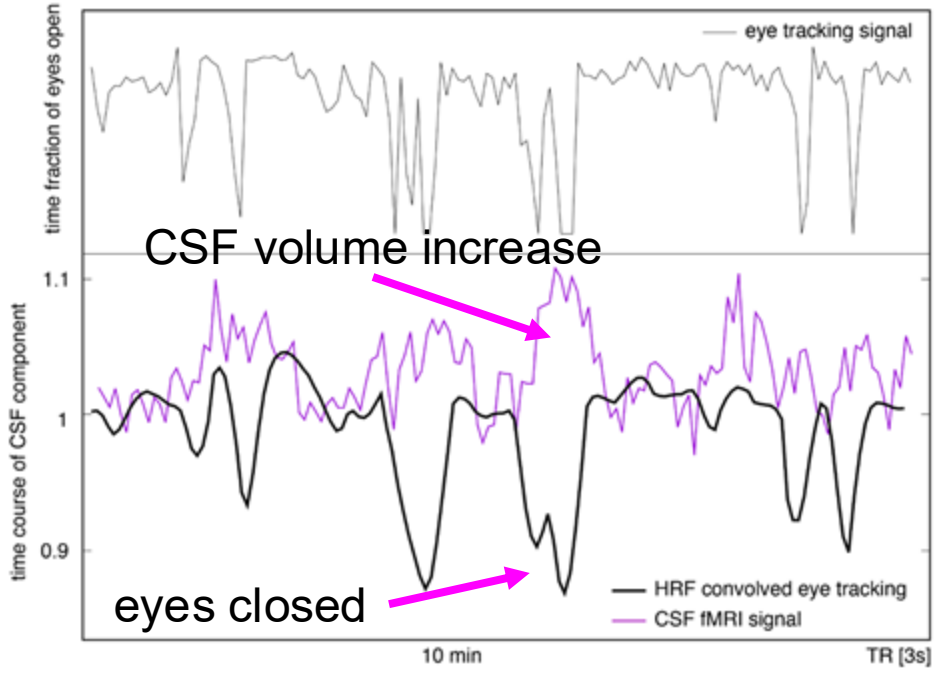

As eyes get more drowsy, CSF volume increases

CSF and CBV correlates of alertness

Preliminary maps of CSF and CBV correlates of alertness

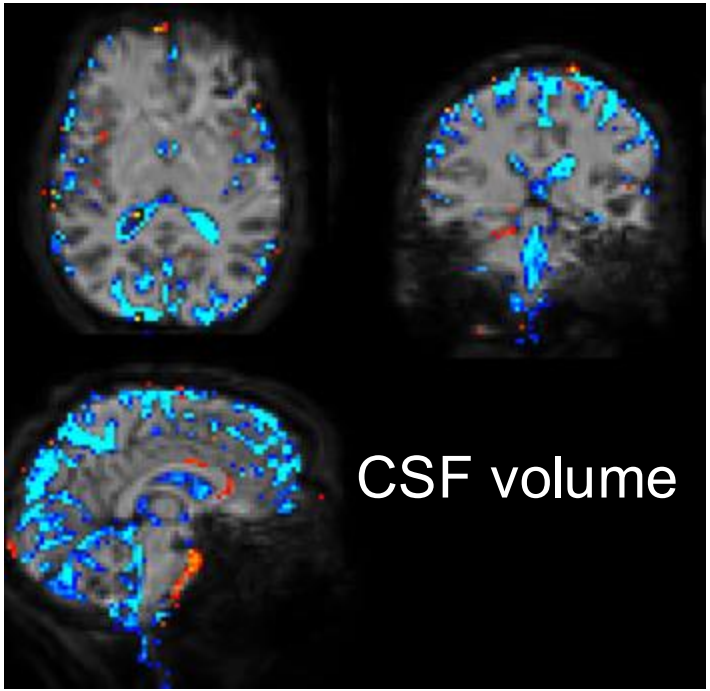

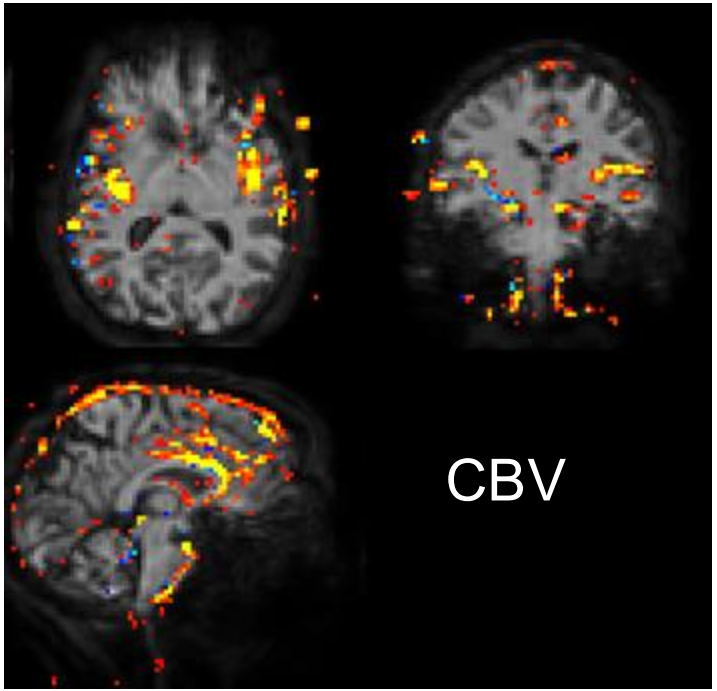

CSF shows a decrease with alertness and CBV shows an increase with alertness

Summary and Conclusion

- We developed a multi-echo multi-inversion fMRI sequence that is simultaneously sensitive to CSF volume, CBV and BOLD.

- We see indications of CSF volume change during functional activation. And even more so during changes of drowsiness.

- Future work will include further validations of the Bloch model (converting 9 TI-TE combinations → CSF, CBV, BOLD) with ground truth CSF modulation tasks.

Thank you!

Than you to Michael Reel, Brittany Pollard and Shruti Japee for their help with participant scheduling logistics.

Thank you to everyone in the Section on Functional Imaging Methods (SFIM), The FMRI Facility (FMRIF) and the layer-FMRI working group for their help and feedback on this project.

We thank César Caballero-Gaudes and Burak Akin for helpful discussions.

The research was conducted as part of the NIMH/NINDS Intramural Research Program (#ZIAMH002783, #ZICMH002884).
MRI scanning was performed in the FMRIF core.

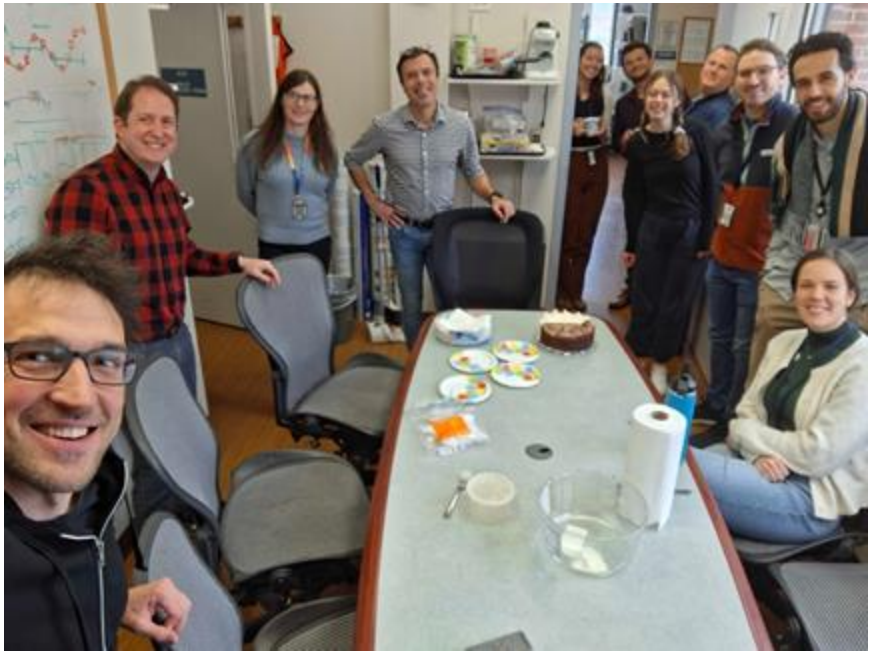

References

- Fultz, Nina E et al. “Coupled electrophysiological, hemodynamic, and cerebrospinal fluid oscillations in human sleep.” Science (New York, N.Y.) vol. 366,6465 (2019): 628-631. doi:10.1126/science.aax5440
- Kim, J.-H., Im, J.-G., & Park, S.-H. “Measurement of CSF pulsation from EPI-based human fMRI.” Neuroimage 257 (2022): 119293. https://doi.org/10.1016/j.neuroimage.2022.119293
- Grubb, S., Lauritzen, M., 2019. Deep sleep drives brain fluid oscillations. Sci New York N Y 366, 572–573. doi:10.1126/science.aaz5191
- Gonzalez-Castillo, J., Fernandez, I.S., Handwerker, D.A., Bandettini, P.A., 2022. Ultra-slow fMRI fluctuations in the fourth ventricle as a marker of drowsiness. NeuroImage 259, 119424. https://doi.org/10.1016/j.neuroimage.2022.119424
- Scouten, A., Constable, R.T., 2008. VASO-based calculations of CBV change: Accounting for the dynamic CSF volume. Magnetic Resonance in Medicine 59, 308–315. https://doi.org/10.1002/mrm.21427
- Stirnberg, R., Stöcker, T., 2021. Segmented K-Space Blipped-Controlled Aliasing in Parallel Imaging (Skipped-CAIPI) for High Spatiotemporal Resolution Echo Planar Imaging. Magnetic Resonance in Medicine 85, 1540–1551. https://doi.org/10.1101/2020.06.08.140699
- Huber, Renzo. “Mapping Human Brain Activity by Functional Magnetic Resonance Imaging of Blood Volume.” 2014. Universität Leipzig. https://ul.qucosa.de/landing-page/?tx_dlf[id]=https%3A%2F%2Ful.qucosa.de%2Fapi%2Fqucosa%253A13259%2Fmets
- Huber, Laurentius., Goendr, Jozien., Kennerley, Aneurin J., Ivanov., Dimo. Krieger, Steffen N., Lepsien, Jöran., Trampe, Robert., Turner, Robert., Möller, Harald E. “Investigation of the Neurovascular Coupling in Positive and Negative BOLD Responses in Human Brain at 7T.” https://eprints.gla.ac.uk/93359/1/93359.pdf
- Ivanov, D., Schäfer, A., Deistung, A., Streicher, M.N., Kabisch, S., Henseler, I., Roggenhofer, E., Jochimsen, T.H., Schweser, F., Reichenbach, J.R., Uludag, K., Turner, R., 2013. In vivo estimation of the transverse relaxation time dependence of blood on oxygenation at 7 tesla. In Proceedings of the 21st Annual Meeting of ISMRM, Salt Lake City, Utah, USA. p. 2472.
- Donahue, M.J., Hoogduin, H., van Zijl, P.C., Jezzard, P., Luijten, P.R., Hendrikse, J., 2011. Blood oxygenation level-dependent (BOLD) total and extravascular signal changes and DeltaR2* in human visual cortex at 1.5, 3.0 and 7.0 T. NMR Biomed. 24, 25-34. doi: 10.1002/nbm.1552
- Jessen NA, Munk AS, Lundgaard I, Nedergaard M. The Glymphatic System: A Beginner's Guide. Neurochem Res. 2015 Dec;40(12):2583-99. doi: 10.1007/s11064-015-1581-6. Epub 2015 May 7. PMID: 25947369; PMCID: PMC4636982.
- Jin, T., Kim, S.G., 2010. Change of the cerebrospinal fluid volume during brain activation investigated by T1 ρ-weighted fMRI. NeuroImage 51, 1378–1383. https://doi.org/10.1016/j.neuroimage.2010.03.047